Control of an Electromagnetic Linear Actuator Using Flatness Property and Systems Inversion

Paolo Mercorelli * **Kai Lehmann** * **Steven Liu** † **Husam Muamer** * **Bernd Reimann** *

* Institut für Automatisierung und Informatik
Schlachthofstr. 4
D-38855 Wernigerode
Germany
Tel. +49-(0)3943-6259746
mercorelli@iai-wr.de

† Harz University of Applied Studies and Research
Friedrichstraße 57-59
D-38855 Wernigerode
Germany
Tel. +49 (0)3943-659332
sliu@hs-harz.de

Keywords: Electromagnetic linear actuator, flatness based control, inverse systems, robust control.

Abstract

The paper presents a robust tracking controller design for a short-stroke permanent magnet motor as a linear drive. After the model description, a flatness based control is presented to force the system following a reference trajectory. Additionally, a robust feedback control, based on system inversion, is used to stabilize the tracking against external disturbance signals, model and initial errors. Moreover, a particular PID control scheme is proposed by using Karitonov's approach.

1 Introduction and motivation

As an important mechatronic component electromagnetic actuators are widely used in many industrial applications. For linear motion control more and more mechanical or hydraulic-mechanical components have been replaced by electromagnetic devices due to their high efficiency, excellent dynamic behavior and small size. In combination with microprocessor control high dynamic and high precision movement can be efficiently realized by such mechatronic actuators. Generally, there is a large variety of different electromagnetic actuators for linear motions, for instance in [2, 5, 6]. For long strokes AC linear motor concept is often preferred while for micro and nano meter applications special designs based on piezoelectric or magnetostrictive principles have been frequently investigated. For moving distances between 5 and 20 mm, however, DC linear motors have proven to be advantageous [2]. This paper considers a DC permanent magnet linear motor which is based on the voice coil principle with low mass and high dynamic. The objective of this paper is to show the controller design scheme for tracking of smooth motion trajectory. Section 2 is devoted to the model description and problem statement. In section 3 some structural properties of the system, such as flatness, input and disturbance relative degrees, are shown. A strategy of control is derived in section 4. The simulation results close the paper.

2 Model Description

Fig. 1 shows the geometry of the permanent magnet linear motor investigated. The geometry is based on an axis-symmetric design. The device consists of an outer and an inner iron part. Permanent magnets are mounted on the inner iron parts. Their magnetization is indicated by the element arrows. The coils are placed within the air gap, between the permanent magnets and the outer iron part. They are connected in series and fed by a variable voltage source. Linear motion is engaged due to the Lorentz force produced in the coils. The coils form the moving part of the actuator and will be referred to the armature in the following sections.

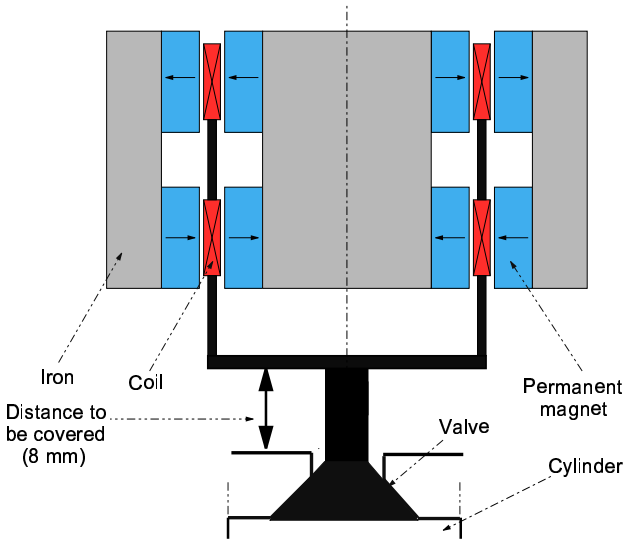

Figure 1: Design principle of the linear motor

Linear actuators based on the principle described above are usually called voice-coil motors. They are especially designed to have a very high dynamic due to its high force and low mass.

In the application reported here we developed such an actuator to quickly control a gas valve over a distance of about 8 mm within a few milliseconds, while the effective length of the whole actuator is about 100 mm and the its diameter about 50 mm. Besides the very high acceleration required for the application large gas pressures against the motion while opening the valve have to be taken into account as system disturbance. These gas pressures, resulting in a disturbance force of some hundred Newton, depend on the changing states of the physical system and are not predictable. Furthermore, soft-landing in case of valve closing is an important issue as well.

2.1 Electrical circuit of the linear motor

The electrical circuit of the actuator can be described by the well known coil equivalent circuit in Fig. 2. The coils are connected in series. Since the permanent magnets are polarized inversely[1], the coils also have to be winded inversely in order to produce Lorentz force in one common direction. The electrical

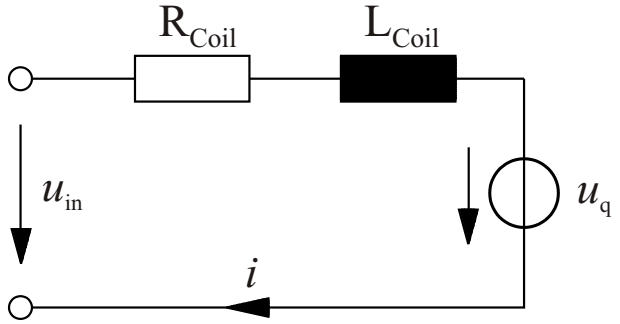

Figure 2: Electrical equivalent circuit of the actuator

system is given by

$$u_{\text{in}} = R_{\text{Coil}} i + L_{\text{Coil}} \dot{i} + u_{\text{q}} \tag{1}$$

where u_{in} represents the input voltage, i the coil current and R_{Coil} and L_{Coil} the resistance and the inductance of the coil windings. The inductance is depending on the armature position and can be derived from finite-element analysis. The induced voltage

$$u_q = l B_g v \tag{2}$$

is generated due to the armature speed v. In equation 2, parameter l represents the coil lead length and B_g represents the magnetic flux density in the air gap which is a function of both the armature position and the coil current. A vectorial expression of the induced voltage is not required since the geometry boundaries are perpendicular, see Fig. 1. Equation 1 can be written in state-space representation

$$\dot{i} = -\frac{R_{Coil}}{L_{Coil}} i + \frac{u_{in} - u_q}{L_{Coil}} \tag{3}$$

in order to provide the first system equation for assembling the complete model.

[1] when seen in direction of movement

2.2 Magnetic circuit of the linear motor

Since the actuator has an axis-symmetric design, half of the geometry can be used for magnetic modelling. An equivalent magnetic circuit diagram is used in order to determine the magnetic quantities of the actuator. Fig. 3 shows the equivalent magnetic circuit diagram of one half of the linear motor (compare to the geometry, Fig. 1). The magnetic flux within the

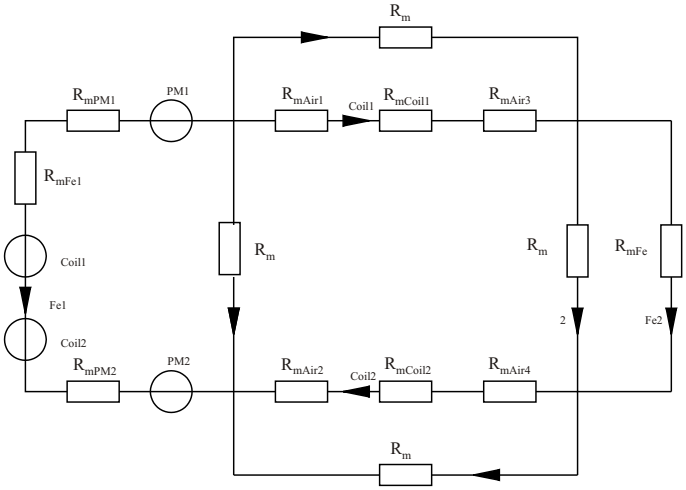

Figure 3: Equivalent magnetic circuit of the linear motor

actuator is inhomogenous. The application of linear magnetic circuit diagram is usually only correct to homogenous fields. However, by defining a precise circuit diagram and by tuning this diagram according to a finite-element program, correct results can be obtained. Four leakage reluctances approximate the leakage flux within the actuator. These are placed at the air paths around the coils. Rather than determining the leakage reluctances analytically we used finite-element analysis in order to obtain realistic leakage reluctance figures. The coils magnetic sources

$$\Theta_{Coil} = Ni, \tag{4}$$

where i represents the coil current and N the number of windings, act on the inner iron part. However, their magnetic resistance takes effect in the air gap. Since the coils are winded inversely (see subsection 2.1), their generated magnetic flux also propagates inversely. The calculation of the magnetic reluctances R_m in Fig. 3 is based on equation 5 (well known from magnetic fundamentals).

$$R_m = \frac{l_m}{\mu A}, \tag{5}$$

where l_m is the magnetic flux path, μ the permeability and A the cross-section area through which the flux penetrates. The magnetic voltage source Θ_M of the permanent magnet is determined by

$$\Theta_M = H_c h_m \tag{6}$$

where H_c is the coercive force of the permanent magnet and h_m its width in direction of polarization.
The magnetic equivalent circuit in Fig. 3 can be solved by using Kirchoff's laws, for instance. As the result, the magnetic

fluxes Φ of the circuit are available. Having derived the magnetic fluxes in Fig. 3, the flux densities

$$B = \frac{\Phi}{A} \tag{7}$$

are calculated. From the calculation of the flux densities within the air gap, the forces are used as input signals for the mechanical system, which will be shown in the next subsection. In order to provide updated permeability-data for the nonlinear iron parts, the field strength

$$H_{Fe} = \frac{V_{Fe}}{l_{phiFe}} \tag{8}$$

in the iron parts has to be calculated. Parameter l_{phiFe} represents the magnetic flux path in the iron. The magnetic potentials V_{Fe} in the iron parts are given by

$$V_{Fe} = R_{mFe}\Phi_{Fe} \tag{9}$$

The values H_{Fe} can be derived from BH-saturation curves.

2.3 Mechanical circuit of the linear motor

The mechanical system is given by

$$0 = F_L - F_a - F_{fric} + F_0, \tag{10}$$

where F_L represents the Lorentz force

$$F_L = lB_g i \tag{11}$$

and F_0 stands for the disturbance force acting on the armature. As mentioned before this disturbance force can have a very high value (up to 400 N) compared to the relatively small size of the actuator. However, this disturbance decays rapidly after the valve has been opened slightly. In a first approximation the disturbance force can be modelled as a reducing exponential function with unpredictable amplitude and time constant. Because of this large disturbances and also parameter uncertainties due to the nonlinear magnetic conditions a robust control is required to ensure the overall system stability. The viscose friction force F_{fric} can be derived from

$$F_{fric} = K_d v, \tag{12}$$

where K_d is the damping coefficient and v is the velocity of the moving part of the actuator. The force required for acceleration is given by

$$F_a = ma, \tag{13}$$

where m is the mass of the moving part and a its acceleration. The mechanical system can be set up in state-space representation

$$\frac{F_L - F_{fric} + F_0}{m} = a = \dot{v} = \ddot{s}, \tag{14}$$

with the actuator position s, in order to provide to complete the system equations for describing the linear motor.

2.4 Assembly of the system equations

Having shown the modelling of the actuator in the previous sections the model's system equations can be summarized as follows:

$$\dot{i} = -\frac{R_{Coil}}{L_{Coil}} i + \frac{u_{in} - lB_g(s,i)v}{L_{Coil}} \tag{15}$$

$$\dot{s} = v \tag{16}$$

$$\dot{v} = lB_g(s,i)i + \frac{-K_d v + F_0}{m} \tag{17}$$

Equation (15) represents the electrical system of the actuator. Equations (17) and (16) both describe the mechanical behavior of the actuator, where equation (17) also contains the magnetic system. The system equations are nonlinear due to the saturation of the iron materials and the leakage fluxes.

3 Some structural properties

In many industrial applications the linear movement along a reference trajectory is desired, even in presence of perturbations like parameter uncertainties and external disturbances. The generation of such a reference trajectory can follow some special aspects of system consideration like the smoothness of the motion or minimization of the loss energy. Moreover, online adaption of reference trajectory is also often considered in connection with some overall control strategies (e.g. adaptive or predictive control). For the considered application, another system property, namly soft-landing of the valve, is required to ensure a long operation life. This means that the armature velocity is to be kept less than some pre-defined value (in our case about 0.1 m/s) when the actuator comes to the end position and no overshoot is allowed.

The system described in Fig. 1 and represented by the mathematical relationships (15), (16) and (17) presents some structural properties which should be useful to perform the control system.

3.1 Flatness based control

Roughly speaking, a system is differentially flat if it is possible to find a set of outputs equal in number to the number of inputs, such that all states and inputs are expressed in terms of those outputs and their derivatives. To be more precise, if the system has state variables $\mathbf{x} \in \Re^n$, and inputs $\mathbf{u} \in \Re^m$ then if the system is flat then the outputs $\mathbf{y} \in \Re^m$ have the following form

$$\mathbf{y} = \mathbf{y}(\mathbf{x}, \mathbf{u}, \dot{\mathbf{u}}, \ldots, \mathbf{u}^p) \tag{18}$$

and

$$\mathbf{x} = \mathbf{x}(\mathbf{y}, \dot{\mathbf{y}}, \ldots, \mathbf{y}^q); \quad \mathbf{u} = \mathbf{u}(\mathbf{y}, \dot{\mathbf{y}}, \ldots, \mathbf{y}^q). \tag{19}$$

Differentially flat systems are useful in situations where explicit trajectory tracking is required. Since the behavior of the flat system is given by the flat output, it is possible to plan

trajectories in output space, and then map these to appropriate inputs. The basic approach of two degrees of freedom design is to initially separate the nonlinear controller synthesis problem into design of a feasible feedforward tracking control for the nominal model of the system, followed by a feedback regulation around that trajectory using controllers which guarantee performance in the presence of uncertainties. The splitting of the problem in two steps has several advantages. The method allows to design advanced controllers which help to achieve robust performance.
In order to show that our system represented by (15), (16) and (17) is ¤at, we choose the position s as the "guess-output", then

$$y = s \Rightarrow s = y, \quad \dot{s} = \dot{y}, \tag{20}$$

$$i = \frac{1}{lB_g(s,i)}(\frac{k_d}{m}v + \dot{v}) \tag{21}$$

and

$$u_{in} = -L_{Coil}\dot{i} + R_{Coil}i + u_q \tag{22}$$

The condition required in (19) is satisfied. The relationships (21) and (22) define the inverse magneto-mechanical and electrical systems respectively. According to the flatness of the system the linearizing trajectory of the model (16) and (17) is the following,

$$i_d = \frac{1}{lB_g(s,i)}(\frac{k_d}{m}\dot{s}_d + \ddot{s}_d),$$

where s_d is the desired trajectory and i_d the desired coil current. The next step is to build a control law which, in presence of external disturbances and uncertainties on the parameters, keeps the system around the desired trajectory.

3.2 Input and disturbance relative degrees

For sake of simplicity, the standard Lie derivative notation is used, see [3]. For a vector $\mathbf{x} \in \Re^n$, a real-valued function $h(\mathbf{x})$ and a vector field $\mathbf{f}$, the derivative of $h(\mathbf{x})$ along $\mathbf{f}$ is denoted by

$$L_{\mathbf{f}}h(\mathbf{x}) = \sum_{i=1}^{n} \frac{\partial h(\mathbf{x})}{\partial x_i} f_i(x) = \frac{\partial h(x)}{\partial(\mathbf{x})}\mathbf{f}(\mathbf{x}).$$

The function

$$L_{\mathbf{g}}L_{\mathbf{f}}h(\mathbf{x}) = \frac{\partial L_{\mathbf{f}}h(\mathbf{x})}{\partial \mathbf{x}}\mathbf{g}(\mathbf{x})$$

means taking the derivative of h first along a vector field $\mathbf{f}(\mathbf{x})$ and then along a vector field $\mathbf{g}(\mathbf{x})$. The function $L^i_{\mathbf{f}}h(x)$ satisfies the recursion relation

$$L^i_{\mathbf{f}}h(\mathbf{x}) = \frac{\partial L^{i-1}_{\mathbf{f}}h(\mathbf{x})}{\partial \mathbf{x}}\mathbf{f}(\mathbf{x})$$

with $L^0_{\mathbf{f}}h(\mathbf{x}) = h(\mathbf{x})$. In particular, suppose that the dynamic system is representable in the following way

$$\dot{\mathbf{x}} = \mathbf{f}(\mathbf{x}) + \mathbf{g}(\mathbf{x})u(t) + \mathbf{p}(\mathbf{x})d(t), \tag{23}$$

where $\mathbf{x}$ is the state vectors, $\mathbf{f}(\mathbf{x})$ is the vectorial map of the dynamic of the system, $\mathbf{g}(\mathbf{x})$ and $\mathbf{p}(\mathbf{x})$ are the vectorial map of the input and of the disturbance respectively. To be more precise, in our presented case

$$\mathbf{f}(\mathbf{x}) = \begin{pmatrix} \frac{-R_{Coil}}{L_{Coil}}i \\ v \\ lB_g(s,i)i + \frac{-K_d}{m}v \end{pmatrix}, \ \mathbf{g}(\mathbf{x}) = \begin{pmatrix} \frac{-1}{L_{Coil}} \\ 0 \\ 0 \end{pmatrix},$$

$$\mathbf{p}(\mathbf{x}) = \begin{pmatrix} 0 \\ 0 \\ \frac{-1}{m} \end{pmatrix}.$$

Definition 1 *The nonlinear system represented in (23) has input relative degree equal to r if*

$$L_{\mathbf{g}}L^i_{\mathbf{f}}h(\mathbf{x}) = 0 \qquad 0 \le i < r-1, \tag{24}$$

$$L_{\mathbf{g}}L^{r-1}_{\mathbf{f}}h(\mathbf{x}) \neq 0. \tag{25}$$

In the same way, the system has disturbance relative degree equal to r if

$$L_{\mathbf{p}}L^i_{\mathbf{f}}h(\mathbf{x}) = 0 \qquad 0 \le i < r-1, \tag{26}$$

$$L_{\mathbf{p}}L^{r-1}_{\mathbf{f}}h(\mathbf{x}) \neq 0. \tag{27}$$

□

According to the definition, the considered system in (15), (16) and (17), with voltage u_{in} as input, has *input relative degree* equal to 3. Considering F_o as external disturbance, then its disturbance relative degree is 2. Thus, the disturbances rejection can not be reached with Isidori approach as the perfect localization of the disturbance in the zero dynamic of the system is not possible, see [3]. In the following some further considerations regarding the structural properties of the system are shown:

- Input relative degree:

  $h(\mathbf{x}) = s; \ \ \frac{\partial h(\mathbf{x})}{\partial \mathbf{x}} = \begin{pmatrix} 0 & 1 & 0 \end{pmatrix}.$

  $$L_{\mathbf{g}}h(\mathbf{x}) = \begin{pmatrix} 0 & 1 & 0 \end{pmatrix} \begin{pmatrix} \frac{-1}{L_{Coil}} \\ 0 \\ 0 \end{pmatrix} = 0.$$

  It yields with easy calculations $L_{\mathbf{g}}L^2_{\mathbf{f}}h(\mathbf{x}) \neq 0$.

- Disturbance relative degree:

  Considering F_0 as the input disturbance then

  $h(\mathbf{x}) = s; \ \ \frac{\partial h(\mathbf{x})}{\partial \mathbf{x}} = \begin{pmatrix} 0 & 1 & 0 \end{pmatrix}.$

$$L_{\mathbf{p}}h(\mathbf{x}) = \begin{pmatrix} 0 & 1 & 0 \end{pmatrix} \begin{pmatrix} 0 \\ 0 \\ \frac{-1}{m} \end{pmatrix} = 0.$$

$$L_{\mathbf{f}}h(\mathbf{x}) = \begin{pmatrix} 0 & 1 & 0 \end{pmatrix} \begin{pmatrix} \frac{-R_{Coil}}{L_{Coil}} i \\ v \\ lB_g(s,i)i + \frac{-K_d}{m} v \end{pmatrix} = v.$$

To conclude

$$L_{\mathbf{p}}L_{\mathbf{f}}h(\mathbf{x}) = \begin{pmatrix} 0 & 0 & -1 \end{pmatrix} \begin{pmatrix} 0 \\ 0 \\ \frac{-1}{m} \end{pmatrix} = \frac{1}{m}.$$

Thus, the disturbance relative degree is equal to 2. □

This result shows that a perfect localization of the disturbance through a combination of the state variable is not possible because the disturbance relative degree is less than the input relative degree , see [3].

4 Control law

A linear PID controller is implemented in order to limit the effect of the disturbance without using an estimator of the disturbance. Linear PID controllers are in industrial applications very often used because their low cost and easy implementation. It is straightforward to observe that by applying the equation (22) to the system, in absence of the disturbance and parametric uncertainties, the exact feedforward linearisation is obtained. Now, instead of (22) let us consider the following input for feedback PID control:

$$u_{d^*} = -L_{Coil}\dot{i}_d + R_{Coil}i_d + \lambda_1 \int e_2 dt + \sum_{i=2}^{3} \lambda_i e_i, \quad (28)$$

with $e_1 = i_{Coil} - i_d$, $e_2 = s - s_d$ and $e_3 = v - v_d$. The term u_q (induced voltage) was neglected and $\sum_{i=2}^{3} \lambda_i e_i(t) = \lambda_2(s - s_d) + \lambda_3(\dot{s} - \dot{s}_d)$, with λ_1 and λ_2 two suitable controller parameters. Once x_d is defined, through the equation (21) the desired current is obtained. Using the control law in (28) the structure of the error equation, without considering external disturbances and model uncertainties, becomes the following:

$$\begin{aligned} \dot{e}_1 &= -\frac{\left(R_{Coil}e_1 + \lambda_1 \int e_2 dt + \sum_{i=2}^{3} \lambda_i e_i - lB_g v_d\right)}{L_{Coil}} \\ \dot{e}_2 &= e_3 \\ \dot{e}_3 &= -\frac{k_d}{m}e_3 - \frac{lH_c d_m R_{subs}(s, i_{Coil})}{2A_{Coil}m}e_1, \end{aligned}$$

with $\dot{s}_d = v_d$. From the error structure and through easy calculations it is possible to determinate the constant λ_1, λ_2 and λ_3 such that the error dynamic is stable. More, thanks to the contribution of $\frac{lB_g(s,i_{Coil})}{L_{Coil}} v_d$ on the above equation, it is straightforward to show that, after a transient period, even though in presence of model uncertainties, the position error and the velocity error follow the profile of the desired velocity. As consequence if the parameters λ_1, λ_2 and λ_3 are chosen so that the dynamic is high enough, then at the time t_f, the £nal time of the desired trajectory, almost perfect soft landing is achieved. The case with disturbance opens again the stability problem as in [1]. In fact, because of the presence of the current varying terms the error equation becomes as following:

$$\begin{aligned} \dot{e}_1 &= -\frac{\left(R_{Coil}e_1 + \lambda_1 \int e_2 dt + \sum_{i=2}^{3} \lambda_i e_i - l\Delta B_g v_d\right)}{L_{Coil}} \\ \dot{e}_2 &= e_3 \\ \dot{e}_3 &= -\frac{k_d}{m}e_3 - \frac{lH_c d_m \Delta R_{subs}}{2A_{Coil}m}e_1, \end{aligned}$$

where $\Delta B_g = [B_g^- \quad B_g^+]$ and $\Delta R_{subs} = [R_{subs}^- \quad R_{subs}^+]$ define the boxes which characterize the interval uncertainty and thus represent the so called interval polynomial. Nevertheless, the stability could be analyzed with the well known Kharitonov's Theorem [4]. The error interval polynomial due to the integral differential equation is a polynomial of forth order with two interval boxes, the Kharitonov's stability test involves just four polynomial tests. For sake of brevity the test is not reported here. In a heuristic way also the settling time and the overshot of the error through the bound of the boxes are tested. In fact, it is known that in general functions like settling time and overshot are not convex functions on the bounded boxes.

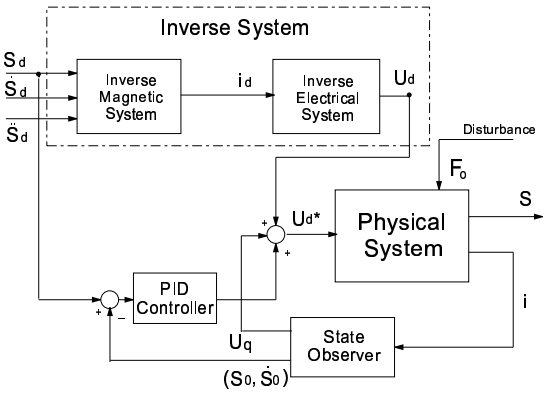

Figure 4: Control scheme.

5 Simulation results

Simulation results are performed by using real actuator data. Tracking of smooth trajectories has been carried out with errors not more than ± 60 micro meters even in presence of high value exponential disturbance force (maximum value equal to 400 N), depicted in Fig. 5. In Fig. 6 some typical simulation results are reported. The performance of the controller is obviously satisfied. It is useful to remark that the simulation is performed without any a-priory knowledge of the disturbance.

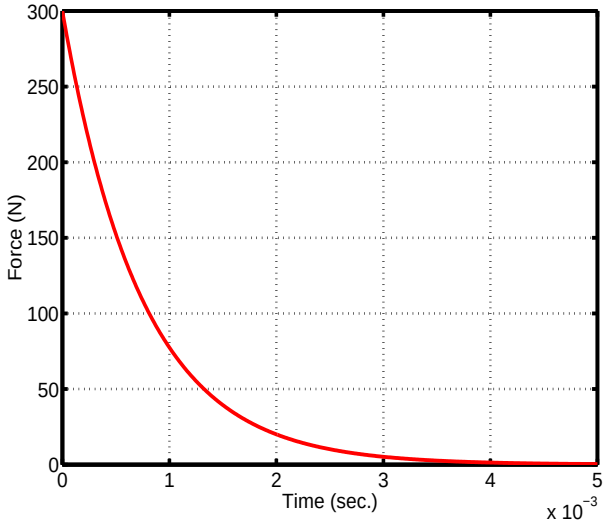

Figure 5: External disturbance.

6 Conclusions

The paper deals with the control design problem based on the flatness property for a permanent magnetic machine. A decentralized inverse model is performed in order to obtain low level of the input control. Classical PID-Controller are adopted to compensate for the perturbation due to the parameter uncertainties and to the large external disturbances without a-priori knowledge. Future works involve a self-tuning of the PID control parameters using observed external disturbance and an overall optimal tracking strategy.

References

[1] V. Hagenmeyer. *Robust nonlinear tracking control*. Fortschritt-Berichte VDI Verlag Reihe 8 Nr. 978, Düsseldorf, 2003.

[2] D. Howe and Z.Q. Zhu. Proc. status of linear permanent magnet and reluctance motor drives in europe. *LDIA'98*, pages 1–7, 1998.

[3] A. Isidori. In *Nonlinear Control Systems*, Ed. Spring-Verlag, August 1989.

[4] V. L. Kharitonov. Asymptotic stability of an equilibrium position of a family of systems of linear differential equations. *Differentsial'nye Uravneniya*, 14:2086–2088, 1978.

[5] K. Lehmann. *Modellierung elektromagnetischer Linearaktuatoren als Ventiltrieb*. Diplomarbeit Hochschule Harz, 2002.

[6] P. Mercorelli, S. Liu, and S. Braune. A geometric approach by using switching and ¤atness based control in electromechanical actuators for linear motion. In *Proccedings 6th International Conference on Mechatronics Technology*, pages 64–69, Kitakyushu (Japan), 2002.

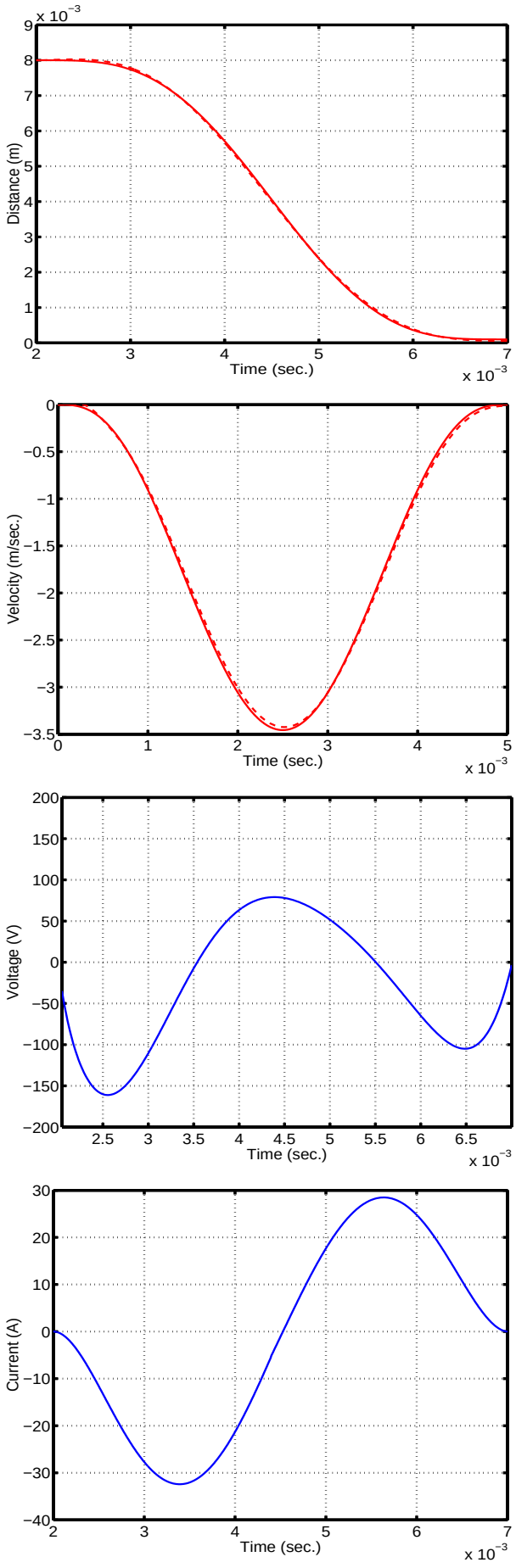

Figure 6: Picture I: desired/obtained trajectory (solid/dasched line). Picture II: desired/obtained velocity (solid/dasched line). Picture III: Input voltage. Picture IV: Currents.